

High Resolution Mapping of Nitrate Loads of a Reservoir Using an Uncrewed Surface Vehicle:  
Potential opportunities and Challenges

Kwang-Hun Lee<sup>1</sup>, Shahid Ali<sup>1</sup>, Yena Kim<sup>1</sup>, Kitack Lee<sup>1,2</sup>, Sae Yun Kwon<sup>1,2</sup>, Jonghun Kam<sup>1,2\*</sup>

21 October 2023

<sup>1</sup>Division of Environmental Science and Engineering, Pohang University of Science and  
Technology, Pohang, South Korea

<sup>2</sup>Institute for Convergence Research and Education in Advance Technology, Yonsei University,  
Seoul, South Korea

\*Corresponding author:

Dr. Jonghun Kam ([jhkam@postech.ac.kr](mailto:jhkam@postech.ac.kr))  
Division of Environmental Science and Engineering  
Pohang University of Science and Technology  
Pohang, South Korea 37673  
Phone: +82-54-279-2318  
Fax: +82-54-279-8299

Key Points:

- An uncrewed surface vehicle (USV) was used to map water depth and nitrate concentration at a 10-meter resolution.
- Nutrient load estimates varied up to 17% when comparing the USV method to a point-measurement method.
- Limitations and challenges of USV-based surveys for water quantity and quality were discussed.

## Abstract

Reliable nutrient load estimation of a reservoir is challenging due to inconsistent spatial extent and temporal frequency of water quality and quantity. This study aims to collect consistent spatial extent and temporal frequency of water depths and nitrate concentrations of a reservoir in South Korea using uncrewed surface vehicle (USV). In this study, reservoir nitrate loads were estimated using four methods to examine how spatial variation in water depth and nitrate concentrations affected load estimates. Based on dual measurements of water depth and nitrate concentration, reservoir nitrate loads across 30 sampling dates (0.7 million tons of fresh water on average) ranged from one to four tons. Results showed that a point measurement of water depths and nitrate concentrations can cause up to –17% of underestimation of nitrate loads, particularly after intense rainfall events. This study highlights potential opportunities and challenges of the USV-based dual monitoring systems for water quality and quantity.

## Plain Language Summary

Water quantity and quality are monitored at different spatial extent and temporal frequency. This study used an uncrewed boat to measure the water depth and nitrate concentration of a reservoir in the mid-eastern Korean Peninsula at considering the spatial component and temporal components. This uncrewed boat was equipped with water depth and nitrate concentration sensors. During the study period (2021–2022), uncrewed boats conducted 30 surveys. We found strong seasonal variations in nitrate load estimates in the reservoir, particularly during the wet season. These results suggest that estimating nitrate loads from depth measurements at a point measurement in a reservoir can lead to underestimates. This study is a case study how the cutting-edge technologies like our uncrewed boat equipped with environmental sensors can be used for the next-generation water monitoring system.

## 1. Introduction

Nitrate is derived from natural and anthropogenic inputs via nutrient deposition from the atmosphere (Kim et al., 2011; Kim et al., 2014; Liu et al., 2013). Lakes and reservoirs have been used to monitor changes in inland nitrate deposition, which can affect their aquatic ecosystems (Elser et al. 2009). Such a nutrient regime shift in lakes and reservoirs via atmospheric deposition may change the structure of aquatic ecosystems and threaten the biodiversity (Folke et al., 2004). The water depth or water storage volume of a reservoir can affect water quality and is controlled by precipitation and water usage. Water quantity and quality of reservoirs are strongly associated with each other, particularly during the wet/dry season (Larsen et al., 1999). Monitoring changes in water depth and nitrate concentration of lakes and reservoirs requires a holistic monitoring system of hydroclimatological variables including precipitation, temperature, and biogeochemical transformations (e.g., assimilation and denitrification; Kendall et al., 2007; Pellerin et al., 2014).

Strong seasonality has been often reported in the water depth, water storage volume, shape, size, and ecology of a reservoir, which can affect nutrient mixing process and may lead to harmful algal blooms (Feyisa et al., 2014; Pekel et al., 2016). Hydroclimatic extremes, such as droughts and floods, can show clear interactions of water quality and quantity. A severe drought increases the nitrate concentration and the hydraulic residence time in the aquatic system (Beklioglu et al., 2008). As air temperature increases and long hydraulic residence time, water temperature also increase enhancing stratification in freshwater systems. (Baldwin et al., 2008). This may lead to toxic cyanobacterial blooms and lowered dissolved oxygen concentrations

(Chapra, 1997). Reduced flushing and enhanced productivity also elevate nutrient, turbidity and algal levels (Mosley, 2015). This environment can trigger eutrophication and cause catastrophic impacts on the aquatic ecosystem (Zhang et al., 2018). Heavy rainfall increases surface runoff and non-point pollutant transports from the surrounding areas of the reservoir into the aquatic systems (Golladay et al., 2002). Furthermore, environmental incidents can degrade significantly the water quality, causing a lack of available water resources and increasing negative complaints regardless of the amount of water resources (Liu et al., 2023). While degraded water quality may restrict availability for certain purposes, such as recreational activities, it may still be suitable for other critical applications like flood control (Cao et al., 2021). Therefore, both water quality and quantity indices can help monitor the availability of water resources accurately with spatially and temporally consistent measurement of water quantity (Yu et al., 2016), which is crucial for proactive management of water resources (Cao et al., 2021).

Water quantity and quality have been monitored at inconsistent sampling frequencies and site locations worldwide. For example, the water level of a reservoir is measured hourly, and the water quality is monitored at weekly or longer. These different sampling frequencies of water quality and quantity of the reservoir are a potential source of uncertainties in assessing the availability of water resources (water quantity: Faro et al., 2019; Gosling and Arnell, 2016; Luo et al., 2020; water quality: Al-Omran et al., 2015; Schoumans et al., 2014; Reynolds et al., 2016; Cassidy and Jordan., 2011). Over the last decade, new technologies have been implemented for efficient water quality monitoring and bathymetric surveys. A low-cost probe with multiple electrochemical sensors can monitor water quality parameters at once in real time. The field deployment of this multiple parameter probe at a gauge site showed acceptable agreement in temperature, specific conductance, pH, and DO between the EXO sondes and the site sonde (Snazelle, 2015). This probe has been used to construct a real-time water quality monitoring system with the Internet of Things (IoT) technology over estuarine and urban areas, employing a combination of stationary and mobile sensors installed in multiple locations (Demetillo et al., 2019; Méndez-Barroso et al., 2020; Irvine et al., 2022).

A bathymetric sensor, Acoustic Doppler Current Profiler (ADCP), has implemented for measurement of water quantity and speed along streams and over lakes and oceans. The ADCP measures the water depth and absolute current speed along the water column up to one-kilometer depth at the hyper spatial resolution (vertical: up to 0.2 meters; Fong et al., 2006; Brown et al., 2011; Li et al., 2018). The ADCP transmits "pings" of sound at a constant frequency into the water. A high frequency pings of the ADCP yields more precise data, but it runs out of batteries rapidly, and accuracy degradation of the ADPC is caused by attenuation of the signal noise ratio between water and transducer due to air entrainment (Fujii et al., 2022). Water quality sensors have been mounted on a boat to map horizontal variation of water quality (Gruberts et al., 2012; Crawford et al., 2015). Potential opportunities of high-resolution mapping through a remotely operated vehicle of water quality along rivers were explored in early 2010s (Casper et al., 2012). Recently, uncrewed underwater and surface vehicles have been used for water quality mapping, particularly for mixing processes of water (Amran et al., 2020; Honek et al., 2020; Griffiths et al., 2022). Surveys of these vehicles are cost efficient to maintain and measure water quality and quantity regularly (e.g., sub-weekly and weekly intervals). These uncrewed vehicles with water quality sensors and ADCP offer a new opportunity to understand interactions of water quality and quantity in aquatic environments. However, applications of these cutting-edge technologies to dual monitoring of water quality and quantity along river streams and in reservoirs remains limited.

Recently, the government of South Korea government enacted the Framework Act on Water Management (FAWM). The FAWM aimed to develop the national dual monitoring system of water quantity and quality. The FAWM system can monitor water quantity and quality along river streams or at lakes and reservoirs at the consistent sampling time and frequency. Despite such administrative efforts, the application of dual monitoring techniques for water quantity and quality along rivers and in reservoirs remains lacking and this study is an attempt to fill this gap.

This study uses an uncrewed surface vehicle (USV) with water quality sensor and depth finder to conduct 30 surveys over a year for dual monitoring of water quality and quantity of a small reservoir named Daljeon near the Southeastern coastline of South Korea. This study aims to investigate the importance of the high-resolution mapping of water quality and depth on changes in nitrate load estimates stored in the study reservoir. The USV-based dual monitoring system used in this study is described in the next section. This study attempts to answer the following research questions: 1) To what extent can high-resolution mapping of water quantity and quality improve nutrient load estimates in the Daljeon reservoir? 2) When are the uncertainties in nitrate load estimates large or small over time? 3) What are the key sources of uncertainties in nitrate load estimates? This study was carried out locally; however, the findings of this study will provide an insight of potential opportunities and challenges for application of the current cutting-edge technologies to dual monitoring water quality and quantity, illuminating the potential value of USV-based surveys for the next-generation water resources monitoring system.

## 2. Study site and data

The Daljeon reservoir is used for irrigation in Pohang, South Korea (36.029 °N, 129.293 °E; Figure 1a). This reservoir was built in 1968 to supply water resources only for agriculture during the crop planting and growing seasons (April–August) and has been managed by the Korea Rural Community Corporation (KRCC). The flood water level, average water level, and dead storage level of this reservoir are 47, 44 and 36 elevation meters above sea level, respectively. That is, the maximum and average water depth of the reservoir is 11 and 8 meters. The maximum water storage volume is 698,300 m<sup>3</sup> (<https://rawris.ekr.or.kr/>). The maximum water surface area of the study reservoir is 0.15 km<sup>2</sup>, which is in Level 2 (> 0.1 km<sup>2</sup>) of the Global Lakes and Wetlands Database (GLWD-2; <https://www.worldwildlife.org/pages/global-lakes-and-wetlands-database>). According to the KRCC website, the upstream land use sources include 54% paddy fields, 18% forest, and 30% residential (households). In this study, 30 USV-based surveys for water depth and nitrate concentration have been conducted in the Daljeon reservoir for accessibility to various launching points.

To examine air-water interactions over the reservoir and how environmental factors may affect water quality and quantity, daily precipitation and temperature data (July 2021– August 2022) over Pohang, South Korea are compared with our dual monitoring data for water quality and quantity. The meteorological data are publicly accessible from the Korea Meteorological Administration (KMA) stations (<https://www.kma.go.kr/>). In addition, the KRCC provided daily measured water levels of the reservoir. We aggregated monthly nitrate concentrations of 19 reservoirs and 4 lakes within 100 km from the Daljeon reservoir that were retrieved from the Water Environment Information System (<https://water.nier.go.kr/>). These data were used as a reference for our USV measurements because of their similar land use types (e.g. paddy and forest).

### 3. Materials and Methods

#### 3.1. USV equipped with water quantity and water quality sensors

In this study, SonTek's rQPOD remote control surveying package was used to mobilize the water depth and water quality sensors (Figure 1). The rQPOD modular remote surveying package is an uncrewed surface vehicle (USV), consisting of rQPOD and a floating platform (Figure 1b). The rQPOD is installed on a floating platform and transforms it into a motorized vehicle for remote operation. The rQPOD is controlled by a transmitter, Futaba T6K, at a frequency of 2.4 GHz, range 500 meters (Figure 1f). The USV is equipped with a pair of trolling motors, which are located on the bottom edge of both sides (Figure 1c). Our YSI EXO2 was fixed at 10 centimeters depth, and ADCP was fixed at the water surface. The maximum speed of the trolling motors is 1.5 m/s and the minimum depth required for the USV to collect accurate data is approximately one meter. The weight of the floating platform is 4.7 kilograms. The maximum payload capacity of the rQPOD is 28 kilograms. Two DJI Phantom 3 LiPO batteries are used for the rQPOD operation. In this study, a floating platform with rQPOD, batteries, GPS system, telemetry system, ADCP and water quality sensors are approximately 25 kilograms. Detailed specifications of the rQPOD remote control surveying package is found from the SonTek's website (<https://www.ysi.com/rqpod>).

For bathymetric measurement (water depth and velocity), the SonTek HydroSurveyor-M9 Acoustic Doppler Current Profiler (ADCP), the Power/Communication Module (PCM), and the SonTek Real Time Kinematic positioning GPS (RTK GPS) were mounted on the floating platform. The 0.5 MHz vertical beam has an eight-degrees beam angle, which can measure from 0.2 up to 80 m below the water surface (Figure 1e). The 1 MHz and 3 MHz doppler beams (bottom tracking method) are operated with a beam angle of three-degrees, which can measure from 0.2 up to 40 meters below the water surface. The ADCP depth accuracy is  $2 \text{ cm} \pm 1\%$  of the measured depth with the highest resolution of 2 centimeters. RTK GPS provides the geopositioning data (longitude, latitude, and altitude) of the USV with a horizontal accuracy of less than 0.03 m (Figure 1g). PCM supports power for ADCP and RTK GPS, using 16 units of double-A batteries. It can transmit the measured data from ADCP and RTK GPS to the home station laptop using telemetry operated at a frequency of 2.4 GHz. The range of the PCM telemetry system is up to 500 meters. During the site surveys, the telemetry system for data transmission was 200-300 meters.

In addition, the YSI EXO2 multi-parameter sonde (EXO2) was mounted on the USV to measure multiple water quality variables every second (Figure 1d). The EXO2 was installed with sensors for *in situ* monitoring such as water temperature (T), pH, electro conductivity (EC), dissolved oxygen (DO), and nitrate ( $\text{NO}_3^-$ ) concentration. The YSI EXO nitrate smart sensor ranges from 0 to 200 mg/L, and the precision is  $\pm 10\%$  of reading or 2 mg/L. The sensor is able to detect 63% of the change in the nitrate concentration level within less than 30 seconds (Response time:  $T_{63} < 30 \text{ sec}$ ; <https://www.ysi.com/product/id-599709/exo-nitrate-smart-sensor>). The monitoring data can be logged internally on the YSI handle for on-site monitoring. The nitrate concentration is measured using ion selective electrodes (ISE). Silver/silver chloride (Ag/AgCl) wire electrodes are used in the nitrate ISE sensor, which is filled with a filling solution. A polymer membrane separates the filling solution from the sample medium, and this membrane interacts with nitrate ions. The ratio of nitrate in the sample to the internal filling

solution affects the electrical potential created across the membrane when the nitrate sensor is placed in water. This potential difference is then measured using a pH reference electrode. (Capelo et al., 2007)

### 3.2. Sampling Survey Schedules

Thirty sampling surveys were conducted in the Daljeon reservoir from July 2021 through August 2022 (Figure 2). Survey paths were determined by the meteorological conditions of the sampling date and spatial coverage was prioritized, and we allowed for inconsistent sampling paths because of limitations of the battery power of the trolling motors. The USV used in this study is recommended to navigate when the wind speed is less than 8 m/s. The limitations of our USV are addressed in more detail in the discussion section. These sampling survey dates and IDs are shown in Table 1. We conducted the surveys between 12:00 and 15:00 on each survey date to minimize potential variations of environmental conditions. The USV was launched from a location in the southwest part of the reservoir. However, vegetation near this launching point often blocked the view and the connectivity between the boat and remote controller. After October, 1, 2021 (ID 6–30), the USV was launched at the docking spot of the eastern part of the reservoir, which allowed us to survey the water quantity and quality over a broader region than before. While the official battery duration of rQPOD was four to six hours without instruments (nine kilograms), our USV's battery lifetime was 20–30 minutes because the weight of our USV was almost three times higher than the floating platform with rQPOD. The official battery duration of rQPOD was four to six hours without instruments (nine kilograms). The weight of our USV was almost three times higher than the floating platform with rQPOD. The USV's battery lifetime was 20–30 minutes during the early survey dates (ID1-10) when the two units of the batteries were used. Since November 5, 2021 (ID 11), the power system was changed with the six units of the batteries of the rQPOD to conduct a one hour-long sampling survey. The remaining 20 % of the northern and western parts of the reservoir were not surveyed because they were shallow (less than one meter). While the official specification of the PCM connection range is 200–300 meters, the connection range of our USV varied, depending on the meteorological conditions.

In the winter of 2021/22 (January 14 and February 11, 2022), the northern and southern parts of the surface in the Daljeon reservoir were frozen. The USV surveyed water depth and quality only over the middle part of the reservoir (ID 16 & 17 in Figure 2). Specific sampling survey schedules and corresponding sampling ID numbers (ID 1–30) were shown in Table 1.

### 3.3. Sensor Calibration

Data logged internally on the YSI handle. According to the EXO2 manual, two-point calibration (1 mg/L and 100 mg/L) was recommended for nitrate concentration calibration. However, this range was too wide to apply in freshwater. In this study, four-point calibration (1, 2, 3, and 4 mg/L) were used. Four-level standard solutions were measured using the YSI EXO2 nitrate sensor over 60 minutes (Figure 3a). The corresponding potentials of 1 mg/L, 2 mg/L, 3 mg/L, and 4 mg/L were  $141.0 \pm 1.8$  mV,  $123.7 \pm 1.4$  mV,  $113.0 \pm 1.1$  mV, and  $104.5 \pm 0.9$  mV, respectively (Fig 3). The potential difference was unstable over 10 minutes after starting measurement. Low variance was observed after 10 minutes (reaching stable conditions). It is worth noting that potential differences before and after stabilization were not large enough (approximately 3-5%) to cross the standard solutions. Using the four-point calibration, three empirical models were applied to find the best-fit model for the relationship of potential

difference and nitrate concentration: linear, logarithm, and exponential (Figure 3c). Based on the R-squared values (Table 2), the exponential model was selected to convert potential difference [mV] to nitrate concentration [mg/L].

Electrochemical sensor measurements are recommended to validate against discrete analytical chemical samples because ion chromatography of standard solutions does not account for the in-situ inferences that are always possible. Cross-validation with discrete analytical chemical samples makes electrochemical sensor measurements reliable, at least in the initial stages of qualifying an autonomous/unscrewed surface vehicles-electrochemical sensor measurement. Discrete analytical chemical samples were not collected during the study period. Instead, the USV-based nitrate concentration measurements were compared with nitrate concentrations from discrete analytical chemical samples near our reservoir, which confirmed that the YSI sensor-based measurements within the nitrate concentration ranges observed in neighboring reservoirs (Figure 7d). Traditional discrete analytical chemical samples at the study site provide a more reliable reference for further studies.

For electrochemical sensor equilibration and ADCP compass calibration, we used measured nitrate concentration and water depth data 10 minutes after launching the USV during each sampling survey. An ADCP compass calibration was performed over the first 10 minutes of each sampling survey to have an accurate track reference. Prior to all ADCP measurements, calibrating the internal magnetic compass of instruments with an external compass is mandatory when using GPS as the navigation reference, to ensure alignment with external compass readings (Mueller and Wagner., 2009). ADCP compass calibrations aim to calibrate out erroneous compass headings caused by sources near the ADCP and the local area.

### 3.4. Nutrient load calculations

The one-second water depth and nitrate data from the USV were used to create 10-meter resolution maps. To quantify the uncertainty of our sampling data from spatial variations, the coefficient of variance (CV) of the nitrate concentration data from each survey is calculated (White et al., 2008). The CV is calculated as the standard deviation divided by the mean of nitrate concentration during each sampling survey. To create the 10-meter filled map, the kriging interpolation method was used to interpolate the measured water depths and nitrate concentrations via the R software “gstat” package (Pebesma and Wesseling, 1998; Gräler et al., 2016). For variogram fitting, we utilized the ‘autofitVariogram’ function from the ‘automap’ package in R, which selected the Matern model with M. Stein's parameterization (Hiemstra et al., 2009). The typical distance between two points is approximately 1.1 meters since the sampling frequency is one second and the average USV speed is 1.1 meters per second. It is worth noting that the distance between two measurement points vary slightly from run to run due to various USV speeds during the survey due to meteorological and water surface conditions.

We tested the sensitivity of volume estimation to spatial variations of water depth and water quality. First, we compared volume estimates using interpolated depths (iD, Eqn. 1) and the mean of depths (aD, Eqn. 2).

$$iD = w \times \sum_{i=1}^N A_i \times d_i \quad (\text{Eqn. 1})$$

, where  $w$  is a weighting parameter for considering unmeasured surface of reservoir ( $w = \frac{A_{\max}(t)}{\sum_i^n A_i}$ ,  $A_{\max}(t) = A_{\max} * \frac{Wl_{\max}(t)}{Wl_{\max}}$ ), where  $A_{\max}$  is actual maximum area of Daljeon reservoir

(151,000 m<sup>2</sup>),  $Wl_{\max}$  is the maximum water level of the study reservoir and  $Wl_{\max}(t)$  is the maximum water level during the sample date.),  $A_i$  is the area of the  $i$ -th grid (constant (100 squared meters))),  $n$  is the number of the 10-meter by 10-meter grids we measured ( $n=1, \dots, N$ ).

$$aD = w \times \bar{d} \times \sum_{i=1}^N A_i \text{ (Eqn. 2)}$$

We also calculated nitrate loads using four different equations. The first equation uses interpolated water depth and interpolated nitrate concentration of a reservoir (iDN, Eqn. 3).

$$iDN = w \times \sum_{i=1}^N (NO_3)_i \times A_i \times d_i \text{ (Eqn. 3)}$$

, where  $(NO_3)_i$  and  $d_i$  were nitrate concentration, and water depth at the  $i^{\text{th}}$  grid, respectively.

The second, third, and fourth equations uses spatial averages of water depths and nitrate concentrations (aDN, Eqn. 4), the interpolated water depths and the spatial averages of nitrate concentrations (iDaN, Eqn. 5), and the spatial averages of water depths and interpolated nitrate concentrations (aDiN, Eqn. 6), respectively.

$$aDN = \bar{d} \times \overline{NO_3} \times \sum_{i=1}^N A_i \text{ (Eqn. 4)}$$

$$iDaN = w \times \overline{NO_3} \times \sum_{i=1}^N A_i \times d_i \text{ (Eqn. 5)}$$

$$aDiN = w \times \bar{d} \times \sum_{i=1}^N (NO_3)_i \times A_i \text{ (Eqn. 6)}$$

$$\Delta D = \frac{aD - iD}{iD} \times 100 \text{ (Eqn. 7)}$$

$$\Delta DN_j = \frac{dDN_j}{iDN} \times 100 \text{ (Eqn. 8)}$$

,where  $j$  depicts the index of the difference of other nitrate load calculation methods from the "iDN" method (aDN, iDaN, aDiN–iDN for  $j=1, 2$ , and  $3$ , respectively).

### 3.5. Comparison spatial resolutions

In this study, a 10-meter spatial resolution was initially selected. The manufacturer recommended USV speed is 1.5 m/s, and the response time of YSI nitrate smart sensor (T63) is less than 30 seconds. Taking these specifications in accounts, 30- and 50-meter resolutions were chosen because the average of the USV speed was around 1.11 m/s, ranging from 0.52 m/s (ID 5) to 1.62 m/s (ID 16). Given the range of USV's speed, a 30-meter resolution is suitable for the most consistent sampling surveys (1.11m/s  $\times$  30 seconds). For the sensitivity test, we compared nitrate concentration maps at 10, 30, and 50-meter resolutions.



## 4. Results

### 4.1. Spatial variation of water depth and nitrate concentration

The CV of nitrate concentration was calculated over the sampling survey dates (Figure 4). The values of CV ranged between 0.02 (ID 30) and 0.18 (ID 11). The mean of CV values in entire period were calculated  $0.09 \pm 0.04$  (mean  $\pm$  standard deviation). In ID 18 and 30, CV values were less than other surveys (CV of ID 18: 0.03, CV of ID 30: 0.02). During these sampling survey dates, the survey time was short (ID 18: 13 minutes, ID 30: 22 minutes) than other sampling survey dates (the sampling survey time average: 47.95 minutes). CVs were higher in the first part of the sampling period (prior to January 2022). Furthermore, the correlation analysis is conducted to examine the relationship between the CV of nitrate concentration and other environmental and survey parameters, such as water temperature, one-week accumulated precipitation, sampling time, travel distance (not shown). The variable with a marginal correlation is water temperature ( $r = -0.31$ ,  $p = 0.08$ ). This result indicates that the CV of nitrate concentration is independent with environmental and sampling parameters.

Spatial variations of water depths of the reservoir resembled the bathymetry of the bottom of the reservoir (Figure 5). The northern and western part of this reservoir were shallower than the middle part of the reservoir. The edges of reservoir were too shallow for the USV to survey the water depth and nitrate concentration. In addition, aquatic plants and debris in the edges made USV difficult to navigate. Moreover, vegetation and debris in the edges of the reservoir made USV difficult to navigate. The spatial variance of nitrate concentrations was relatively weak compared with those of water depths (Figure 6). It is worth noting that the vertical gradient of temperature and nitrate concentration was not measured since this study aimed to investigate the impact of horizontal resolution of the mapping of water quality and quantity. These results indicate temporal changes of spatial variance of nitrate concentrations across the seasons (Figure 6).

### 4.2. Seasonal variations of water temperature, water depth, and nitrate concentration

Pohang has strong seasonal variability of precipitation and temperature (Figure 7). During the study period (July 2021–August 2022), the total precipitation was 1,430.2 millimeters. While the accumulated precipitation was 650.4 millimeters (47%) in July and August of 2021, the total precipitation was 202.1 millimeters from June through August, 2022.

The mean water depth ranged between 3.4 meters (ID 29) and 7.8 meters (ID 3) (Figure 7c). The surveys in the late August and September, 2021 (ID 3-5) covered a larger area in the southern part of the reservoir compared to the surveys in July and early August (ID 1 and 2). The water levels of the Daljeon reservoir were well matched with our measured maximum water depth, particularly during the sampling surveys on August 27, 2021 (ID 3) and January 14, 2022 (ID 15). From ID 1 to ID 3, the mean of water depth increased because of antecedent rainfall events. After the summer of 2021 (ID 3), the mean water depth declined monotonically until the winter of 2021/22 (ID 22), following the decreased patterns of precipitation and air temperature. After ID 22 (May 2022), the water depth decreased gradually, possibly to meet an increasing water demand for agriculture due to lack of rainfall in the spring of 2022.

### 4.3 Sensitivity test of water volume estimation and nitrate storage estimation

The water volume estimates in the reservoir followed the patterns of water depths (Figure 8 (a)). The mean and standard deviations of water volumes from the iD method were

696,037 and 200,614 m<sup>3</sup>, respectively. The estimated water volumes from the iD method ranged between 249,788 m<sup>3</sup> (ID 30) and 1,017,161 m<sup>3</sup> (ID 8). The mean and standard deviations of water volumes from the aD method were 656,958 and 189,394 m<sup>3</sup>, respectively, with a range between 255,144 m<sup>3</sup> (ID 29) and 1,004,085 m<sup>3</sup> (ID 3). The difference between estimated water volumes of iD and aD ( $\Delta D$ ) ranged between -17 % (ID 9) and +2 % (ID 30), confirming that the impact of using the spatially varying data on the water volume estimate of the reservoir. We also found that the one-site measurement of water depth can underestimate the water volume of the reservoir (Figure 8b).

Before the survey on October 29, 2021 (ID 10), the differences of estimated water volumes from the  $\Delta D$  ranged from -17.07 % and -0.13 % with the average difference, -8.10 %. After the survey ID 10, the differences of estimated water volumes from the  $\Delta D$  method ranged -7.66 % to +2.65 % with the averaged difference, -3.95 %. For example, the mean of sampling time is 1,465 and 2,981 seconds before and after the ID 10 survey, respectively. The average estimated areas are 32,000 and 49,500 m<sup>2</sup>, respectively before and after the ID 10 survey (the surveyed grid numbers are 11 and 20).

The estimated nitrate loads in the water reservoir had similar pattern with estimated water volumes (Figure 8c). The estimated nitrate loads from the iDN method ranged from 0.32 (ID 30) to 3.83 tons (ID 19) with the average  $2.09 \pm 1.01$  tons (mean  $\pm$  standard deviation,  $n = 30$ , ton is metric ton). The estimated nutrients from the aDiN method ranged from 0.31 (ID 30) to 3.57 (ID 19) tons with the average,  $1.97 \pm 0.96$  ton ( $n = 30$ ). The estimated nitrate loads from the iDaN method ranged between 0.32 (ID 30) and 3.84 tons (ID 19) with the average,  $2.09 \pm 1.02$  tons ( $n = 30$ ). The estimated water volumes from the aDN method ranged between 0.31 (ID 29) and 3.58 tons (ID 19) with the average,  $1.98 \pm 0.97$  tons ( $n = 30$ ).

The difference between estimated nitrate loads of iDN and iDaN ( $\Delta DN_2$ ) ranged from -6.51 % (ID 1) to +2.65 % (ID 15) with and the average difference, -0.23 % (Figure 8d). The  $\Delta DN_3$  ranged from -16.80 (ID 9) % to +2.79 (ID 30) % with the average difference of -5.93 %. The  $\Delta DN_1$  was calculated in the range of -17.11 (ID 5) % to 3.23 (ID 30) %, and the mean of  $\Delta DN_1$  was -5.64 %. The difference between  $\Delta DN_2$  was smaller than other differences.

## 5. Discussion

### 5.1 Drivers of nitrate variation

This study found a temporal regime shift in the spatial variance of nitrate concentrations between December and January (Figure 6). After January, 2022 (ID 16), CVs in the nitrate concentration estimates declined, and the nitrate concentration estimates showed a low spatial variance over the rest of the sampling survey dates. In November and December of 2021 (ID 10 to ID 15), the CVs increased. In this study, the vertical gradient of nitrate concentrations was not measured, which might induce uncertainties in nitrate load estimation. However, the proposed near surface concentration-based nitrate load calculation in this study were likely a conservative estimate (a lower boundary estimate) because it was previously found that the deep-water nitrate concentration in a reservoir is higher than surface water nitrate concentration (Paerl et al., 1975; Andersen, 1982). Thus, changes in the vertical distribution of nitrate, with depth playing a significant role, could be a factor influencing the observed CV dynamics.

The USV-based sampling data showed temporal changes of spatial variance of nitrate concentrations across the seasons. After heavy rainfall (ID 3), the nitrate concentration increased dramatically (from 1.07 to 3.53 mg/L). The result indicates potential non-point nutrient inflows

from surrounding areas after heavy rainfall events (Uttormark et al., 1974; Zhao et al., 2022). The highest recorded precipitation rate during these storms was 43.1 mm/hour on August 24, 2021. In the summer of 2022, however precipitation was not intense to increase nitrate concentration in the reservoir through non-point nutrient inflows. Assessment of the threshold precipitation value for triggering non-point nitrate inflows still remains limited, which can provide an actionable information for an effective water and land management, particularly the control of nutrient inflows.

The nitrate concentration estimates a high-to-low seasonal regime shift between December and January because horizontal and vertical mixing of lake and reservoir were accelerated by wind speed and air temperature in the winter and spring (Woolway et al., 2020). From sampling surveys during the spring months (ID 17 through ID 19; February to March 2022), the nitrate concentration was high, which is in line with the finding of other sites (Domogalla et al., 1926; Seike et al., 1990). After ID 19, the nitrate concentration began to decrease. Potential causes of the decreased nitrate concentrations are a denitrification and biological removal of nitrate concentration during the spring and summer months. In the Daljeon reservoir, algal blooms were observed visually in summer 2021 and spring 2022, and nutrient concentration were related with algal biomass (Smith, 1982; Paerl et al., 2001). It is known that the biological removal rate of nitrate concentration is also affected by water temperature (Hamilton and Scdhladow, 1997). Another possible cause is the sinking of nutrient to the bottom sediment (Chapra, 1982). In July and August of 2021, intense rainfall events visually increased the turbidity from suspended sediment and increased nitrate concentration by measurement. However, in the summer of 2022, precipitation was not enough to increase nitrate concentration in the reservoir (average daily precipitation in summer 2021: 10.84 mm/day, in summer 2022: 2.25 mm/day). These results confirmed the importance of precipitation intensity on non-point nitrate transports.

This study found that the disparity in  $\Delta DN2$  was notably less pronounced than other variations. It implied that more accurate water volumes at the high spatial resolution play a dominant role in nitrate storage estimation than high-resolution nitrate concentration measurement. However, the resolution of nitrate concentration sampling is significant, depending on the season and the characteristic of a reservoir and surrounding environments. The Daljeon reservoir is relatively small and has the spatially homogeneous spatial distribution of nitrate concentration (Figure 6), resulting in a dominant role of water depth in nitrate load estimation.

## 5.2 Limitations of the USV approach

Our USV has encountered several fundamental limitations. The first limitation is the limited spatial coverage due to the battery lifespan (< 1.5 hours) and floating debris. Given the average navigation speed (1.1 m/s), the USV can travel over the lake up to around six kilometers of the survey path. Intense rainfalls bring a significant amount of floating debris into the lake, which is various, depending on the season and precipitation intensity (Anderson and Sitar, 1995; Yuan et al., 2005). For example, the ID 29 and 30 surveys measured the water quality and depth over relatively small areas of the lake mainly due to floating debris from antecedent significant precipitation and runoff. We faced challenges in collecting accurate data from ID 1 to ID 10, resulting in low confidence in our interpolations. This limitation arose because the battery life of our USV was shorter than specified by the manufacturer. To overcome this issue, we added four additional batteries for sampling after ID 10. Instead of discarding the data prior to ID 10, we

chose to report it with low confidence to share our experiences and the progress made with this technology. Another limitation we encountered was the inability to collect homogeneous and regular data. The manufacturer of the rQPOD, our USV, provides an auto-navigation technology. We attempted to utilize this feature for sampling. However, we faced challenges such as having to replace batteries midway due to their short life, as well as issues with the USV's movement caused by wind and debris (minor environmental problems). As a result, we relied on a remote controller for data collection and made efforts to maintain a consistent and regular path for the boat. Overall, we acknowledge the technical limitations we faced with our USV and have made various adjustments and adaptations to address these challenges.

The interpolation-based spatial maps have uncertainties related to the estimation of the actual water surface area of the study reservoir on the sampling date. In this study, the actual water surface area on the was calculated by multiplying the ratio of the maximum water surface area to the maximum water level by the maximum water level during the sampling date. The proposed method might not capture a complex bathymetry of the reservoirs (see Figure 5). To reduce these uncertainties, combining USV-based surveys with other new technologies, such as drones and remotely operated vehicles, is required (Song et al., 2023). Recently, three dimensional (3-D) lake topography modeling and deep learning techniques with UAV-captured imagery data have been applied to estimate the water surface area and water volume in a reservoir/pond (Fang et al., 2023; He et al., 2023). Our results showed that there were low CV values and weak spatial nitrate variations over the entire study period, except for the fall, indicating that the reservoir undergoes a strong mixing event once a year, suggesting a monomictic lake. To understand mixing processes, the vertical measurement of nitrate concentrations is required, which can be measured by autonomous underwater vehicles (Merrifield et al., 2023).

The YSI nitrate smart sensor, while effective, has certain inherent limitations regarding accuracy and response time. To address these challenges, we have developed an innovative approach to sensor calibration and validation. Traditionally, using these sensors in the field has been problematic when it comes to verifying measured concentrations (Aubert et al., 2014; Rode et al., 2016a; Rode et al., 2016b). Previous research has attempted to validate the sensors through lab experiments (Capelo et al., 2007; Bowling et al., 2016). However, this conventional approach requires additional equipment and techniques to measure chemical concentrations (Beaton et al., 2012). Recently, Samuelsson et al. (2023) highlighted that excessive reliance on laboratory measurements can introduce uncertainties due to the nature of laboratory experiments. They found that more consistent calibration can improve accuracy. In our study, we employed ion chromatography to measure standard solutions, and the results aligned well with the intended concentrations of nitrate standard solutions (1, 2, 3, and 4 mg/L). Subsequently, we proposed a sensor calibration and validation method to measure water depths and nitrate concentrations in the Daljeon reservoir. Most of the nitrate concentration measurements were close to the upper bound of the nitrate concentration range among 23 neighboring lakes/reservoirs. These high nitrate concentrations might be caused by multiple sources including more are of paddy in the watershed, more intense farming of the paddy fields, and more accurate estimate of nitrate concentration estimates from high-resolution mapping. To investigate a true cause of these high nitrate concentration estimates, an inter-comparison study with measurements from neighboring lake/reservoirs is necessary. Furthermore, we observed that the concentrations reported by the YSI device were overestimated for standard solution concentrations of 2, 3, and 4 mg/L (Figure 3c). This observation suggests that the two-point sensor calibration (1 and 100 mg/L)

recommended by YSI was not as accurate within lower concentration ranges. Therefore, we propose that our sensor calibration and validation method could be a viable approach to enhance the accuracy of the YSI nitrate smart sensor and other similar ISE sensors.

In this study, the response time of the YSI nitrate sensor ( $T_{63} < 30\text{sec}$ ) was a crucial factor influencing the decision of an appropriate spatial resolution of water depth and nitrate maps. We conducted a sensitivity test to the horizontal spatial resolution of interpolation of water depths and nitrate concentrations on November, 26 2021 (ID 13) and April 22, 2022 (ID 21) when the CVs were higher and lower than the average (0.09 of CV), respectively (0.16 and 0.08 for ID 13 & 21, respectively). The differences of the nitrate load estimates among the 10, 30, and 50-meter resolution maps were clearer on the ID 13 survey compared to the ID 21 survey (Figure 9). For the ID 13 survey, the nitrate load estimates were 2.44, 2.51, and 2.57 tons from the 10, 30, and 50-meter resolution maps, respectively. The 50-meter resolution map overestimated +5% of nitrate load compared to the 10-meter resolution map. On the other hand, the ID 21 survey date with a low CV value showed no significant impact of the horizontal spatial resolution for nitrate load mapping. These results underscore the importance of high spatial resolution mapping on reducing the nitrate load estimate in a reservoir/lake.

### 5.3 Challenges of the USV approach

This study found that USV-based water volume estimates of the Daljeon reservoir was  $696,037\text{ m}^3$  on average over the study period. The maximum water volume estimate was  $1,017,161\text{ m}^3$  in October, 2021 (ID 8), which was larger than the design maximum capacity ( $698,300\text{ m}^3$ ) by 57%. This discrepancy may be attributed to rehabilitation and upgrade of the reservoir. The Daljeon reservoir has been rehabilitated with two maintenance projects in 2015 and 2022. The KRCC local authority confirmed that the 2015 and 2022 projects included the construction of waterways for paddy fields and the construction of an emergency water gate, respectively. Other than these two projects, the KRCC irregularly conducted dredging to manage the reservoirs, but no official records were available before 2012. The findings of this study implied that other reservoirs constructed in the 1960s and 1970s like the Daljeon reservoir might have significant uncertainties in the designed maximum capacity, which requires a regular inspection program for bathymetry survey.

In this study, we monitored water volume and nitrate concentration simultaneously via the USV equipped water depth and quality sensors. Marcé et al. (2016) reported the importance of simultaneous management of water quality variables (chemical) and ecosystem compounds (biological) in lake and reservoir management. Furthermore, Pomati et al. (2016) emphasized the importance of water quantity and biological compounds for lake water managements. Mounting sensors for chlorophyll *a* or fluorescent dissolved organic matter concentrations on the USV will provide important information of interactions between water quantity and quality and their ecological impacts (Bowling et al., 2016; Liu and Georgakakos, 2021).

Recently, the Surface Water and Ocean Topography (SWOT) satellite was launched in December 2022 (<https://swot.jpl.nasa.gov/>). Capabilities of the SWOT mission for terrestrial hydrology were introduced as a global-scale monitoring system of surface water storage change and fluxes at the hyper-resolution (about 50–200 meters) (Biancamaria et al., 2015). While the capability of the SWOT to detect extreme U.S. flood events was reported based on SWOT's orbit ephemeris (Frasson et al., 2019), the SWOT satellite data are required for site-specific validation over not only U.S. but also other countries. It also has uneven temporal sampling of surface water storage change, which requires a combination of in situ data from other sources. This study

hinted how the SWOT satellite data can be facilitated by combining the USV-based measurement as a reference and complementary data source.

## 6. Conclusions

This study succeeded to conduct a one-year long surveys of dual monitoring of water quality and quantity in a small-size monomictic artificial lake in South Korea at a spatiotemporally consistent scale using an uncrewed surface vehicle with ADCP and a probe with multiple environmental electrochemical sensors. This study demonstrated that the nutrient load estimates from a one-site monitoring site can be underestimated compared to those from spatially varying measurements of water quality and depths. This study found that water depth appears to be more important than nitrate concentration in the load estimates. Moreover, this study found that the relative importance of water depth and nitrate concentration on the nitrate load estimation vary temporally when the spatial variability of nitrate concentration is strong, particularly during the winter months when the wind speed is high.

This study examined the applicability and practicability of USV to dual monitoring of water quality and quantity. The one year-long dual monitoring data of water quality and quantity of the Daljeon reservoir proved that the USV with ADCP and electrochemical sensors was a costly efficient tool and a step in the development of future technologies. This study also discussed some limitations and challenges of the dual monitoring system via the USV, ADCP, and YSI electrochemical sensors used in this study. Particularly, the USV technology used in this study had the limited sampling survey time and spatial coverage. This USV employment is one step in the development of future technologies. Combining the USV-based approach with other techniques, such as stationary sensors and uncrewed aerial vehicles, uncertainties in measuring the water surface extent can be reduced.

This study emphasized the importance of an initiative effort to apply cutting-edge technologies on developing the next-generating water monitoring system for nitrate load and further environmental implications. More reliable technologies might be available but high-priced. Research and development budgets should support research opportunities to develop the next-generation water monitoring system, which eventually will provide new challenges and opportunities to investigate the coupled dynamics of water quantity and quality and help develop a more efficient and effective water resources monitoring and management system for sustainable development of our communities.

## Authorship contribution statement

**Kwang-Hun Lee:** Conceptualization, Data curation, Investigation, Formal analysis, Methodology, Software, Validation, Visualization, Writing – original draft, Writing – Review & Editing. **Shahid Ali:** Analysis, Validation, Writing – Review & Editing. **Yena Kim:** Validation, Writing – Review & Editing. **Kitack Lee:** Analysis, Validation, Writing – Review & Editing. **Sae Yun Kwon:** Analysis, Validation, Writing – Review & Editing. **Jonghun Kam:** Conceptualization, Methodology, Funding acquisition, Project administration, Resources, Supervision, Writing – review & editing.

## Declaration of competing interest

The authors declare that they have no known competing financial interests or personal relationships that could have appeared to influence the work reported in this paper.

### **Acknowledgments**

This study was supported by the Basic Research Program through the National Research Foundation of Korea(NRF) funded by the MSIT(NRF-2020R1A4A101881812; NRF-2021M3I6A1086808).

### **Data Availability**

The data and python codes used in the study are available at Harvard Dataverse via <https://doi.org/10.7910/DVN/KBHXBH>.

## References

- Al-Omran, A., Al-Barakah, F., Altuquq, A., Aly, A., & Nadeem, M. (2015). Drinking water quality assessment and water quality index of Riyadh, Saudi Arabia. *Water Quality Research Journal of Canada*, 50(3), 287–296. <https://doi.org/10.2166/wqrjc.2015.039>
- Amran, I. Y., Isa, K., Kadir, H. A., Ambar, R., Ibrahim, N. S., Kadir, A. A. A., & Mangshor, M. H. A. (2020). Development of autonomous underwater vehicle for water quality measurement application. In *Proceedings of the 11th National Technical Seminar on Unmanned System Technology 2019: NUSYS'19*, 139–161. Singapore: Springer Singapore. [https://doi.org/10.1007/978-981-15-5281-6\\_11](https://doi.org/10.1007/978-981-15-5281-6_11)
- Andersen, J. M. (1982). Effect of nitrate concentration in lake water on phosphate release from the sediment. *Water research*, 16(7), 1119–1126. [https://doi.org/10.1016/0043-1354\(82\)90128-2](https://doi.org/10.1016/0043-1354(82)90128-2)
- Anderson, S. A., & Sitar, N. (1995). Analysis of rainfall-induced debris flows. *Journal of Geotechnical Engineering*, 121(7), 544–552. [https://doi.org/10.1061/\(ASCE\)0733-9410\(1995\)121:7\(544\)](https://doi.org/10.1061/(ASCE)0733-9410(1995)121:7(544))
- Aubert, A. H., Kirchner, J. W., Gascuel-Oudoux, C., Faucheux, M., Gruau, G., & Mérot, P. (2014). Fractal water quality fluctuations spanning the periodic table in an intensively farmed watershed. *Environmental Science & Technology*, 48(2), 930–937. <https://doi.org/10.1021/es403723r>
- Baldwin, D. S., Gigney, H., Wilson, J. S., Watson, G., & Boulding, A. N. (2008). Drivers of water quality in a large water storage reservoir during a period of extreme drawdown. *Water research*, 42(19), 4711–4724. <https://doi.org/10.1016/j.watres.2008.08.020>
- Beaton, A. D., Cardwell, C. L., Thomas, R. S., Sieben, V. J., Legiret, F. E., Waugh, E. M., ... & Morgan, H. (2012). Lab-on-chip measurement of nitrate and nitrite for in situ analysis of natural waters. *Environmental science & technology*, 46(17), 9548–9556. <https://doi.org/10.1021/es300419u>
- Beklioglu, M., & Tan, C. O. (2008). Restoration of a shallow Mediterranean lake by biomanipulation complicated by drought. *Fundamental and Applied Limnology*, 171(2), 105. DOI: 10.1127/1863-9135/2008/0171-0105
- Biancamaria, S., Lettenmaier, D. P., & Pavelsky, T. M. (2016). The SWOT mission and its capabilities for land hydrology. *Remote sensing and water resources*, 117–147. [https://doi.org/10.1007/978-3-319-32449-4\\_6](https://doi.org/10.1007/978-3-319-32449-4_6)
- Bowling, L. C., Zamyadi, A., & Henderson, R. K. (2016). Assessment of in situ fluorometry to measure cyanobacterial presence in water bodies with diverse cyanobacterial populations. *Water research*, 105, 22–33. <https://doi.org/10.1016/j.watres.2016.08.051>
- Brown, J., Tuggle, C., MacMahan, J., & Reniers, A. (2011). The use of autonomous vehicles for spatially measuring mean velocity profiles in rivers and estuaries. *Intelligent service robotics*, 4, 233–244. <https://doi.org/10.1007/s11370-011-0095-6>
- Cao, X., Zeng, W., Wu, M., Li, T., Chen, S., & Wang, W. (2021). Water resources efficiency assessment in crop production from the perspective of water footprint. *Journal of Cleaner Production*, 309, 127371. <https://doi.org/10.1016/j.jclepro.2021.127371>
- Capelo, S., Mira, F., & De Bettencourt, A. M. (2007). In situ continuous monitoring of chloride, nitrate and ammonium in a temporary stream: comparison with standard methods. *Talanta*, 71(3), 1166–1171. <https://doi.org/10.1016/j.talanta.2006.06.013>



- Casper, A. F., Dixon, B., Steimle, E. T., Hall, M. L., & Conmy, R. N. (2012). Scales of heterogeneity of water quality in rivers: Insights from high resolution maps based on integrated geospatial, sensor and ROV technologies. *Applied Geography*, 32(2), 455–464. <https://doi.org/10.1016/j.apgeog.2011.01.023>
- Cassidy, R., & Jordan, P. (2011). Limitations of instantaneous water quality sampling in surface-water catchments: Comparison with near-continuous phosphorus time-series data. *Journal of Hydrology*, 405(1–2), 182–193. <https://doi.org/10.1016/j.jhydrol.2011.05.020>
- Chapra, S. C. (1982). A budget model accounting for the positional availability of phosphorus in lakes. *Water Research*, 16(2), 205–209. [https://doi.org/10.1016/0043-1354\(82\)90112-9](https://doi.org/10.1016/0043-1354(82)90112-9)
- Chapra, S.C., 1997. *Surface Water-quality Modelling*. McGraw-Hill Publishers.
- Chien-Yuan, C., Tien-Chien, C., Fan-Chieh, Y., Wen-Hui, Y., & Chun-Chieh, T. (2005). Rainfall duration and debris-flow initiated studies for real-time monitoring. *Environmental Geology*, 47, 715–724. <https://doi.org/10.1007/s00254-004-1203-0>
- Crawford, J. T., Loken, L. C., Casson, N. J., Smith, C., Stone, A. G., & Winslow, L. A. (2015). High-speed limnology: Using advanced sensors to investigate spatial variability in biogeochemistry and hydrology. *Environmental Science & Technology*, 49(1), 442–450. <https://doi.org/10.1021/es504773x>
- Demetillo, A.T., Japitana, M.V. & Taboada, E.B., 2019: A system for monitoring water quality in a large aquatic area using wireless sensor network technology. *Sustain Environ Res* 29, 12. <https://doi.org/10.1186/s42834-019-0009-4>
- Domogalla, B. P., Fred, E. B., & Peterson, W. H. (1926). Seasonal variations in the ammonia and nitrate content of lake waters. *Journal (American Water Works Association)*, 15(4), 369–385. <http://www.jstor.org/stable/41228056>
- Elser, James J., et al. 2009: Shifts in Lake N:P Stoichiometry and Nutrient Limitation Driven by Atmospheric Nitrogen Deposition. *Science*, 326, 835–837, DOI:10.1126/science.1176199
- Fang, C., Lu, S., Li, M., Wang, Y., Li, X., Tang, H. and Ikhumhen, H.O., 2023. Lake water storage estimation method based on similar characteristics of above-water and underwater topography. *Journal of Hydrology*, 618, 129146. <https://doi.org/10.1016/j.jhydrol.2023.129146>
- Faro, G. T. C. D., Garcia, J. I. B., Oliveira, C. D. P. M., & Ramos, M. R. S. (2019). Application of indices for water resource systems stress assessment. *Rbrh*, 24. <https://doi.org/10.1590/2318-0331.241920180106>
- Feyisa, G. L., Meilby, H., Fensholt, R., & Proud, S. R. (2014). Automated Water Extraction Index: A new technique for surface water mapping using Landsat imagery. *Remote sensing of environment*, 140, 23–35. <https://doi.org/10.1016/j.rse.2013.08.029>
- Folke, C., Carpenter, S., Walker, B., Scheffer, M., Elmqvist, T., Gunderson, L. and Holling, C.S., 2004. Regime shifts, resilience, and biodiversity in ecosystem management. *Annu. Rev. Ecol. Evol. Syst.*, 35, 557–581. <https://doi.org/10.1146/annurev.ecolsys.35.021103.105711>
- Fong, D. A., & Jones, N. L. (2006). Evaluation of AUV-based ADCP measurements. *Limnology and Oceanography: methods*, 4(3), 58–67. <https://doi.org/10.4319/lom.2006.4.58>
- Frasson, R. P. D. M., Schumann, G. J. P., Kettner, A. J., Brakenridge, G. R., & Krajewski, W. F. (2019). Will the surface water and ocean topography (SWOT) satellite mission observe floods?. *Geophysical Research Letters*, 46(17–18), 10435–10445. <https://doi.org/10.1029/2019GL084686>

- Fujii, H., Nakamura, T., Sambo, L., Sarann, L., Hoshikawa, K., & Fujihara, Y. (2022). Discharge Measurement and Hydraulic Characteristics in the Tonle Sap River. In *Water and Life in Tonle Sap Lake* (pp. 111-120). Singapore: Springer Nature Singapore.
- Golladay, S.W., Battle, J., 2002. Effects of flooding and drought on water quality in Gulf Coastal Plain streams in Georgia. *J. Environ. Qual.* 31 (4), 1266–1272. <https://doi.org/10.2134/jeq2002.1266>
- Gosling, S. N., & Arnell, N. W. (2016). A global assessment of the impact of climate change on water scarcity. *Climatic Change*, 134, 371–385. <https://doi.org/10.1007/s10584-013-0853-x>
- Gräler, B., Pebesma, E. J., & Heuvelink, G. B. (2016). Spatio-temporal interpolation using gstat. *R J.*, 8(1), 204.
- Griffiths, N. A., Levi, P. S., Riggs, J. S., DeRolph, C. R., Fortner, A. M., & Richards, J. K. (2022). Sensor-Equipped Unmanned Surface Vehicle for High-Resolution Mapping of Water Quality in Low-to Mid-Order Streams. *ACS ES&T Water*, 2(3), 425–435. <https://doi.org/10.1021/acsestwater.1c00342>
- Gruberts, D., Paidere, J., Škute, A., & Druvietis, I. (2012). Lagrangian drift experiment on a large lowland river during a spring flood. *Fundamental and applied limnology*, 179(4), 235–249. DOI : 10.1127/1863-9135/2012/0154
- Hamilton, D. P., & Schladow, S. G. (1997). Prediction of water quality in lakes and reservoirs. Part I—Model description. *Ecological modelling*, 96(1–3), 91–110. [https://doi.org/10.1016/S0304-3800\(96\)00062-2](https://doi.org/10.1016/S0304-3800(96)00062-2)
- He, J., Lin, J., Zhang, X. and Liao, X., 2023. Accurate estimation of surface water volume in tufa lake group using UAV-captured imagery and ANNs. *Measurement*, 220, 113391. <https://doi.org/10.1016/j.measur.2023.113391>
- Hiemstra, P.H., Pebesma, E.J., Twenhöfel, C.J. and Heuvelink, G.B., 2009. Real-time automatic interpolation of ambient gamma dose rates from the Dutch radioactivity monitoring network. *Computers & Geosciences*, 35, 1711–1721. <https://doi.org/10.1016/j.cageo.2008.10.011>
- Honek, D., et al., 2020: Estimating sedimentation rates in small reservoirs - Suitable approaches for local municipalities in central Europe, *Journal of Environmental Management*, 261, 109958. <https://doi.org/10.1016/j.jenvman.2019.109958>
- Irvine, K.N., Chua, L.H.C., Irvine, C.A. (2022). Automated in Situ Water Quality Monitoring—Characterizing System Dynamics in Urban-Impacted and Natural Environments. In: Mustafa, F.B. (eds) *Methodological Approaches in Physical Geography. Geography of the Physical Environment*. Springer, Cham. [https://doi.org/10.1007/978-3-031-07113-3\\_6](https://doi.org/10.1007/978-3-031-07113-3_6)
- Kendall, C., Elliott, E. M., & Wankel, S. D. (2007). Tracing anthropogenic inputs of nitrogen to ecosystems. *Stable isotopes in ecology and environmental science*, 2(1), 375–449. DOI:10.1002/9780470691854
- Kim, I. N., Lee, K., Gruber, N., Karl, D. M., Bullister, J. L., Yang, S., & Kim, T. W. (2014). Increasing anthropogenic nitrogen in the North Pacific Ocean. *Science*, 346(6213), 1102–1106. doi: 10.1126/science.1258396
- Kim, T. W., Lee, K., Najjar, R. G., Jeong, H. D., & Jeong, H. J. (2011). Increasing N abundance in the northwestern Pacific Ocean due to atmospheric nitrogen deposition. *Science*, 334(6055), 505–509. doi:10.1126/science.1206583
- Larsen, S. E., Kronvang, B., Windolf, J., & Svendsen, L. M. (1999). Trends in diffuse nutrient concentrations and loading in Denmark: statistical trend analysis of stream monitoring

- data. *Water science and technology*, 39(12), 197–205. [https://doi.org/10.1016/S0273-1223\(99\)00336-4](https://doi.org/10.1016/S0273-1223(99)00336-4)
- Li, C., Weeks, E., Huang, W., Milan, B., & Wu, R. (2018). Weather-induced transport through a tidal channel calibrated by an unmanned boat. *Journal of Atmospheric and Oceanic Technology*, 35(2), 261–279. <https://doi.org/10.1175/JTECH-D-17-0130.1>
- Liu, A., J. Kam, S. Kwon, and W. Shao, 2023: Monitoring the impact of climate extremes and COVID-19 on statewide sentiment alterations in water pollution complaints, *npj Clean Water*, 6, 29. <https://doi.org/10.1038/s41545-023-00244-y>
- Liu, X., & Georgakakos, A. P. (2021). Chlorophyll a estimation in lakes using multi-parameter sonde data. *Water Research*, 205, 117661. <https://doi.org/10.1016/j.watres.2021.117661>
- Liu, X., Zhang, Y., Han, W., Tang, A., Shen, J., Cui, Z., ... & Zhang, F. (2013). Enhanced nitrogen deposition over China. *Nature*, 494(7438), 459–462. <https://doi.org/10.1038/nature11917>
- Luo, P., Sun, Y., Wang, S., Wang, S., Lyu, J., Zhou, M., ... & Nover, D. (2020). Historical assessment and future sustainability challenges of Egyptian water resources management. *Journal of Cleaner Production*, 263, 121154. <https://doi.org/10.1016/j.jclepro.2020.121154>
- Marcé, R., George, G., Buscarinu, P., Deidda, M., Dunalska, J., de Eyto, E., ... & Jennings, E. (2016). Automatic high frequency monitoring for improved lake and reservoir management. *Environmental Science & Technology*, 50(20), 10780–10794. <https://doi.org/10.1021/acs.est.6b01604>
- Méndez-Barroso, L.A., Rivas-Márquez, J.A., Sosa-Tinoco, I. and Robles-Morúa, A., 2020. Design and implementation of a low-cost multiparameter probe to evaluate the temporal variations of water quality conditions on an estuarine lagoon system. *Environmental Monitoring and Assessment*, 192, 710. <https://doi.org/10.1007/s10661-020-08677-5>
- Merrifield, S. T., Celona, S., McCarthy, R. A., Pietruszka, A., Batchelor, H., Hess, R., ... & Terrill, E. J. (2023). Wide-Area Debris Field and Seabed Characterization of a Deep Ocean Dump Site Surveyed by Autonomous Underwater Vehicles. *Environmental Science & Technology*. <https://doi.org/10.1021/acs.est.3c01256>
- Mosley, L. M., 2015: Drought impacts on the water quality of freshwater systems; review and integration, *Earth-Science Reviews*, 140, 203–214. <https://doi.org/10.1016/j.earscirev.2014.11.010>
- Mueller, D.S., and Wagner, C.R., 2009, Measuring discharge with acoustic Doppler current profilers from a moving boat: U.S. Geological Survey Techniques and Methods 3A–22, 72 p. (available online at <http://pubs.water.usgs.gov/tm3a22>).
- Paerl, H. W., Fulton, R. S., Moisander, P. H., & Dyble, J. (2001). Harmful freshwater algal blooms, with an emphasis on cyanobacteria. *TheScientificWorldJournal*, 1, 76–113. <https://doi.org/10.1100/tsw.2001.16>
- Paerl, H. W., Richards, R. C., Leonard, R. L., & Goldman, C. R. (1975). Seasonal nitrate cycling as evidence for complete vertical mixing in Lake Tahoe, California-Nevada 1. *Limnology and oceanography*, 20(1), 1–8. <https://doi.org/10.4319/lo.1975.20.1.0001>
- Pebesma, E. J., & Wesseling, C. G. (1998). Gstat: a program for geostatistical modelling, prediction and simulation. *Computers & Geosciences*, 24(1), 17–31. [https://doi.org/10.1016/S0098-3004\(97\)00082-4](https://doi.org/10.1016/S0098-3004(97)00082-4)
- Pekel, J. F., Cottam, A., Gorelick, N., & Belward, A. S. (2016). High-resolution mapping of global surface water and its long-term changes. *Nature*, 540(7633), 418–422. <https://doi.org/10.1038/nature20584>

- Pellerin, B. A., Bergamaschi, B. A., Gilliom, R. J., Crawford, C. G., Saraceno, J., Frederick, C. P., ... & Murphy, J. C. (2014). Mississippi River nitrate loads from high frequency sensor measurements and regression-based load estimation. *Environmental science & technology*, 48(21), 12612–12619. <https://doi.org/10.1021/es504029c>
- Pomati, F., Jokela, J., Simona, M., Veronesi, M., & Ibelings, B. W. (2011). An automated platform for phytoplankton ecology and aquatic ecosystem monitoring. *Environmental science & technology*, 45(22), 9658–9665. <https://doi.org/10.1021/es201934n>
- Rode, M., Halbedel née Angelstein, S., Anis, M. R., Borchardt, D., & Weitere, M. (2016b). Continuous in-stream assimilatory nitrate uptake from high-frequency sensor measurements. *Environmental science & technology*, 50(11), 5685–5694. <https://doi.org/10.1021/acs.est.6b00943>
- Rode, M., Wade, A. J., Cohen, M. J., Hensley, R. T., Bowes, M. J., Kirchner, J. W., ... & Jomaa, S. (2016a). Sensors in the stream: the high-frequency wave of the present *Environmental science & technology*. 50(19), 10297–10307 <https://doi.org/10.1021/acs.est.6b02155>
- Samuelsson, O., Lindblom, E. U., Björk, A., & Carlsson, B. (2023). To calibrate or not to calibrate, that is the question. *Water Research*, 229, 119338. <https://doi.org/10.1016/j.watres.2022.119338>
- Schoumans, O. F., Chardon, W. J., Bechmann, M. E., Gascuel-Oudou, C., Hofman, G., Kronvang, B., ... & Dorioz, J. M. (2014). Mitigation options to reduce phosphorus losses from the agricultural sector and improve surface water quality: a review. *Science of the total environment*, 468, 1255–1266. <https://doi.org/10.1016/j.scitotenv.2013.08.061>
- Seike, Y., Kondo, K., Hashitani, H., Okumura, M., Fujinaga, K., & Date, Y. (1990). Nitrogen metabolism in the brackish Lake Nakanoumi. IV. Seasonal variation of nitrate nitrogen. *Japanese Journal of Limnology (Rikusuigaku Zasshi)*, 51(3), 137–147.
- Smith, V. H. (1982). The nitrogen and phosphorus dependence of algal biomass in lakes: An empirical and theoretical analysis 1. *Limnology and oceanography*, 27(6), 1101–1111. <https://doi.org/10.4319/lo.1982.27.6.1101>
- Snazelle, T. T., 2015, Evaluation of Xylem EXO water-quality sondes and sensors: U.S. Geological Survey Open-File Report 2015-1063, 28 p., <http://dx.doi.org/ofr20151063>.
- Song, J., Kam, J., & Jones, S. (2023). Utility of remotely operated underwater vehicle in flood inundation mapping for dam failure: A case study of Lake Tuscaloosa Dam. *River Research and Applications*, 1–14. <https://doi.org/10.1002/rra.4217>
- Uttormark, P. D., Chapin, J. D., & Green, K. M. (1974). Estimating nutrient loadings of lakes from non-point sources. US Government Printing Office.
- White, G. H. (2008). Basics of estimating measurement uncertainty. *The Clinical Biochemist Reviews*, 29(Suppl 1), S53. PMID: 18852859; PMCID: PMC2556585.
- Woolway, R. I., Kraemer, B. M., Lenters, J. D., Merchant, C. J., O'Reilly, C. M., & Sharma, S. (2020). Global lake responses to climate change. *Nature Reviews Earth & Environment*, 1(8), 388–403. <https://doi.org/10.1038/s43017-020-0067-5>
- Yu, S., He, L., & Lu, H. (2016). An environmental fairness based optimisation model for the decision-support of joint control over the water quantity and quality of a river basin. *Journal of Hydrology*, 535, 366–376. <https://doi.org/10.1016/j.jhydrol.2016.01.051>
- Zhang, M., Zhi, Y., Shi, J., & Wu, L. (2018). Apportionment and uncertainty analysis of nitrate sources based on the dual isotope approach and a Bayesian isotope mixing model at the watershed scale. *Science of the Total Environment*, 639, 1175–1187. <https://doi.org/10.1016/j.scitotenv.2018.05.239>

824 Zhao, B., Wong, Y., Ihara, M., Nakada, N., Yu, Z., Sugie, Y., ... & Guan, Y. (2022).  
825 Characterization of nitrosamines and nitrosamine precursors as non-point source pollutants  
826 during heavy rainfall events in an urban water environment. *Journal of Hazardous*  
827 *Materials*, 424, 127552. <https://doi.org/10.1016/j.jhazmat.2021.127552>  
828

## List of Table Captions

Table 1. Sampling survey schedules and corresponding sampling ID numbers (ID 1–30). An asterick depicts the first survey when the power system is changed for increase sampling time of the USV.

Table 2. Estimated parameters of three empirical models for the potential difference-nitrate concentration relation using four-level standard solutions.

## List of Figure Captions

Figure 1. Maps of the Daljeon reservoir in Pohang in South Korea (a) and USV-based survey systems: Uncrewed surface vehicle ((b) & (c): top and bottom view, respectively), multi-parameter sonde (YSI-EXO2) (d), ADCP (e), remote controller (f), and GPS receiver (g). Red and blue circles in (a) depict the launching point of the USV before and after ID 6, respectively.

Figure 2. Maps of the paths of the 30 USV-based surveys in the Daljeon reservoir with 10m x 10m grids.

Figure 3. Measured potential difference of nitrate standard solutions using the YSI nitrate sensor over time a), relationship nitrate concentration with potential difference (b). In (a), red, green, blue, and purple lines depict measured potential difference of the standard solutions at 1, 2, 3, and 4 mg/L of nitrate concentration, respectively. In (b), black solid, gray dash and gray solid lines depict exponential, linear, and logarithm functions, respectively. Measured concentration of nitrate standard solution (x-axis) and from the YSI (y-axis) (c).

Figure 4. Coefficient of variances of nitrate concentration during 30 USV-based surveys. Shaded area colored in gray depict the period of the launching point at the southwestern part of reservoir.

Figure 5. 10-meter resolution maps of water depths of the Daljeon reservoir during 30 USV-based surveys.

Figure 6. 10-meter resolution maps of nitrate concentrations of the Daljeon reservoir during 30 USV-based surveys.

Figure 7. Seasonal variations of meteorological and water surface conditions: air and water temperature in Pohang region and Daljeon reservoir, respectively (a), precipitation in Pohang region (b), water depths (c) and nitrate concentration (d) in the Daljeon reservoir. In (a), red, black, and blue lines depict daily maximum, average, and minimum air temperatures, respectively, and open circles depict measured water temperature. In (c), a red line depicts the maximum water depths measured by KRCC and circle markers and error bars depicts water depth averages and standard deviations measured by USV. In (d), circle markers and error bars depict nitrate concentration averages and the minimum-maximum range measured by USV. Red box plots in (d) depict nitrate concentration of the 23 neighboring lakes.

Figure 8. Temporal variation of water volume and nitrate storage estimation by calculating method (a, c, respectively); (a) circle: water volume estimation using interpolated water depth, grey circle: water volume estimation using mean of water depth (iD), (b) the difference of water volume using interpolated water depth between using mean of water depth ( $\Delta D$ ), (c) nitrate loads using interpolated water depths and nitrate concentrations (iDN), and (d) the difference of nitrate storage using interpolated water depth and interpolated nitrate concentration between other methods (aDN, iDaN, and aDiN–iDN for  $j = 1, 2$ , and  $3$ , respectively). Gray box is period of when we docked the boat on the SW part of reservoir.

Figure 9. Nitrate concentration maps ((a)-(f)) and nitrate load estimates ((g) and (h)) of the ID13 and 21 sampling survey at 10-, 30-, and 50-meter resolutions.

Table 1. Sampling survey schedules and corresponding sampling ID numbers (ID 1–30). An asterick depicts the first survey when the power system is changed for increase sampling time of the USV.

ID	Sampling date	Sampling time [min]	Travel distance [m]
1	July 23, 2021	45.93	1.95
2	July 29, 2021	20.95	1.44
3	August 27, 2021	15.30	1.08
4	September 01, 2021	17.18	1.29
5	September 10, 2021	18.02	0.57
6	October 01, 2021	15.50	1.25
7	October 08, 2021	20.80	1.46
8	October 15, 2021	17.68	1.41
9	October 22, 2021	12.50	0.94
10	October 29, 2021	16.87	1.29
11*	November 05, 2021	63.13	3.77
12	November 19, 2021	67.55	4.61
13	November 26, 2021	46.90	3.80
14	December 10, 2021	37.52	2.79
15	December 24, 2021	59.25	4.77
16	January 14, 2022	15.60	1.52
17	February 11, 2022	39.78	3.25
18	March 11, 2022	13.40	1.02
19	March 25, 2022	70.92	3.98
20	April 15, 2022	49.67	3.54
21	April 22, 2022	60.43	4.49
22	May 06, 2022	60.80	4.40
23	May 20, 2022	88.55	4.03
24	June 03, 2022	29.27	2.21
25	June 17, 2022	47.83	3.60
26	July 01, 2022	55.20	4.20
27	July 19, 2022	58.40	4.51
28	August 12, 2022	38.70	2.95
29	August 25, 2022	68.58	3.45
30	August 26, 2022	22.35	0.83



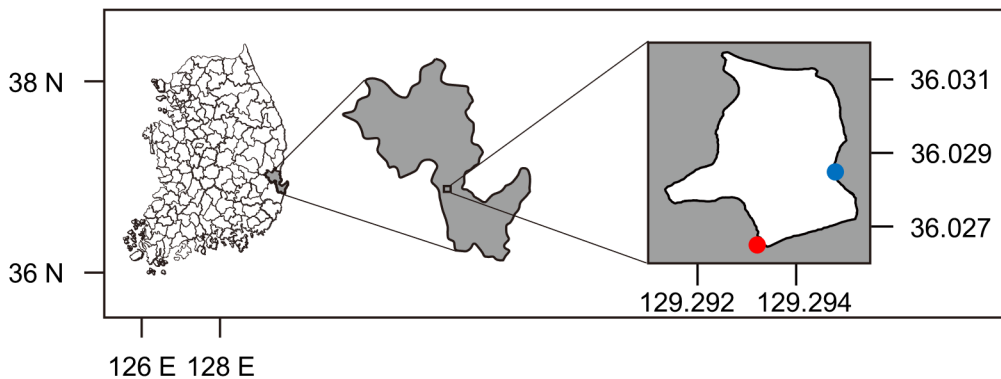
891 Table 2. Estimated parameters of three empirical models for the potential difference-nitrate  
 892 concentration relation using four-level standard solutions.

Line types	Empirical model equation	$R^2$
Linear	$y = -0.08 x + 12.26$	0.972
Logarithm	$y = -9.96 \ln(x) + 50.17$	0.985
Exponential	$y = 221.05 \exp(-0.038x)$	0.998

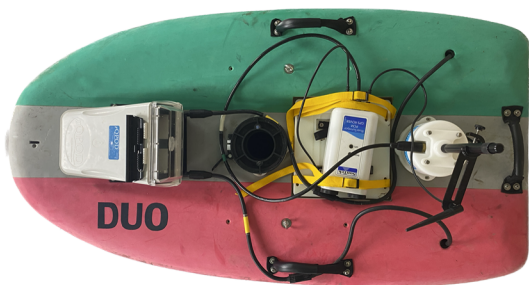
893

Figure 1.

a)



b)



c)



d)



e)



f)



g)



Figure 2.

Latitude

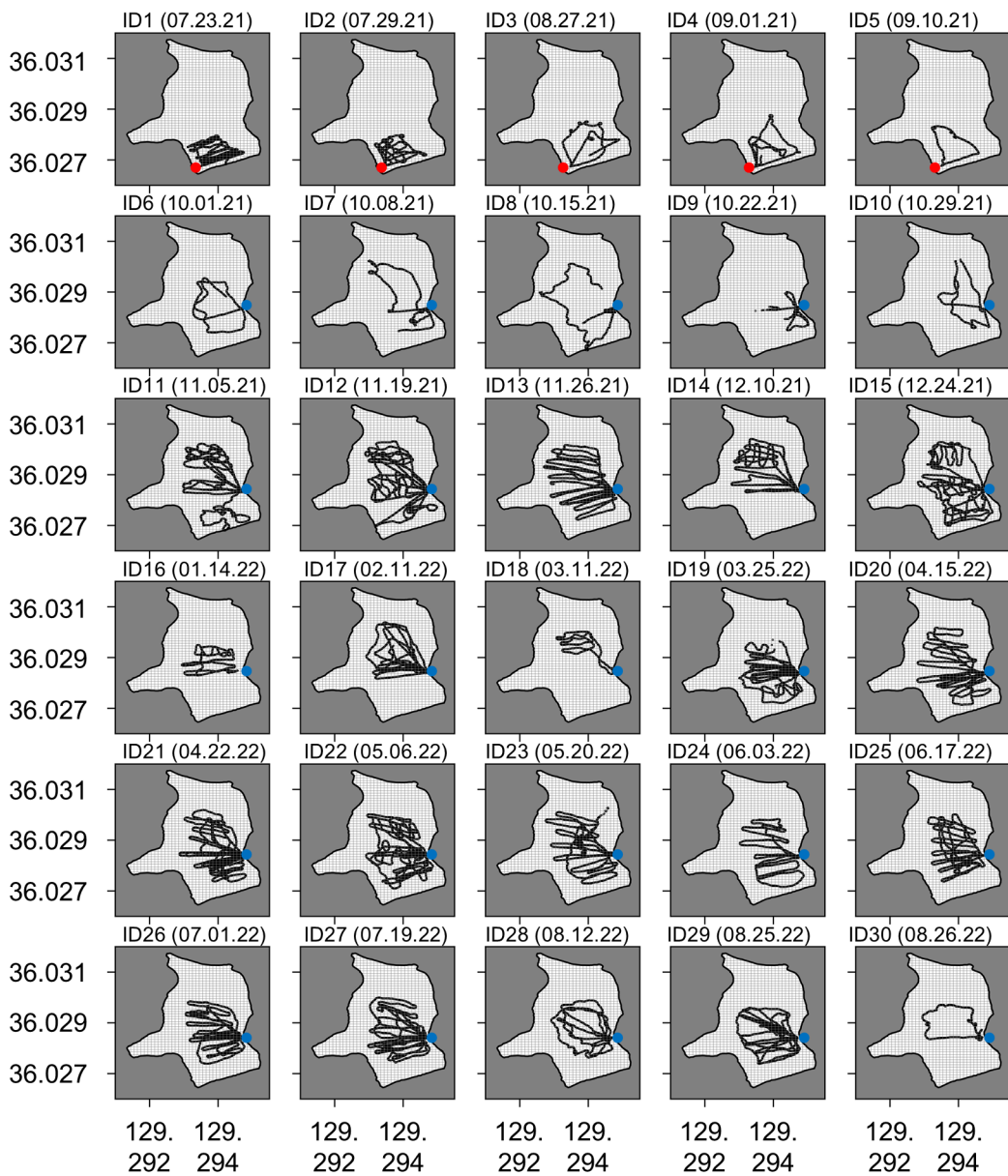


Figure 3.

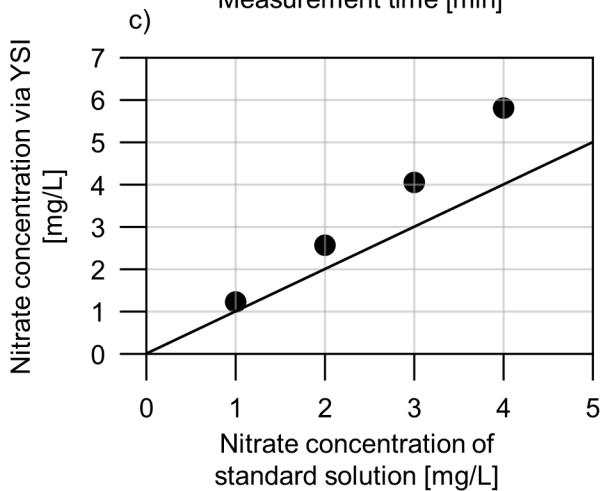
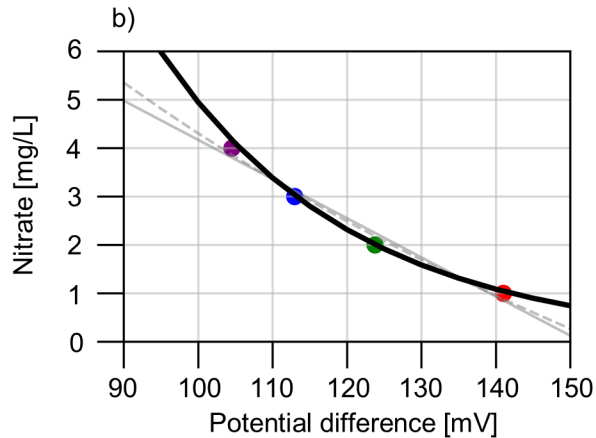
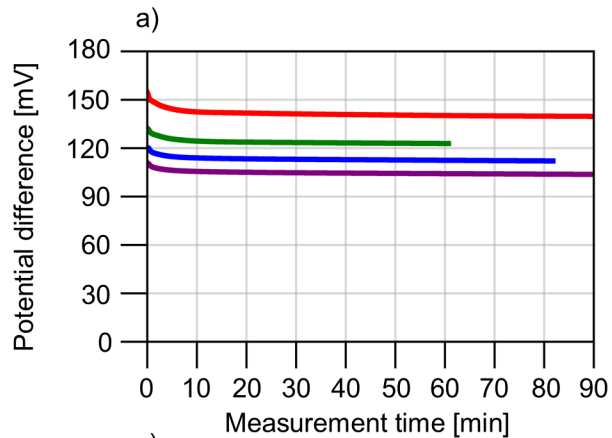


Figure 4.



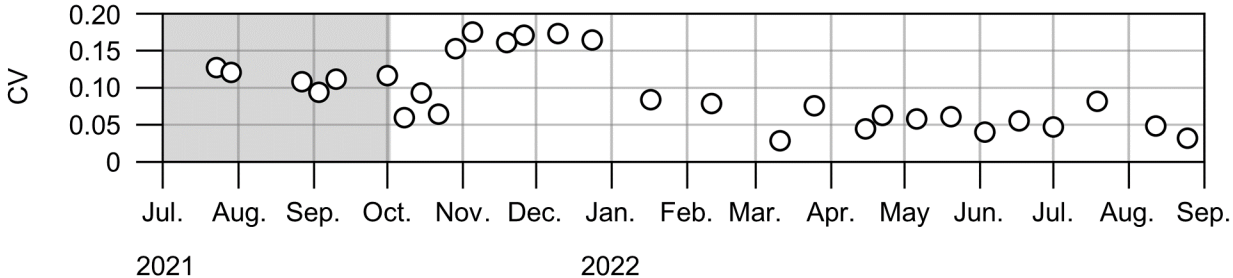


Figure 5.

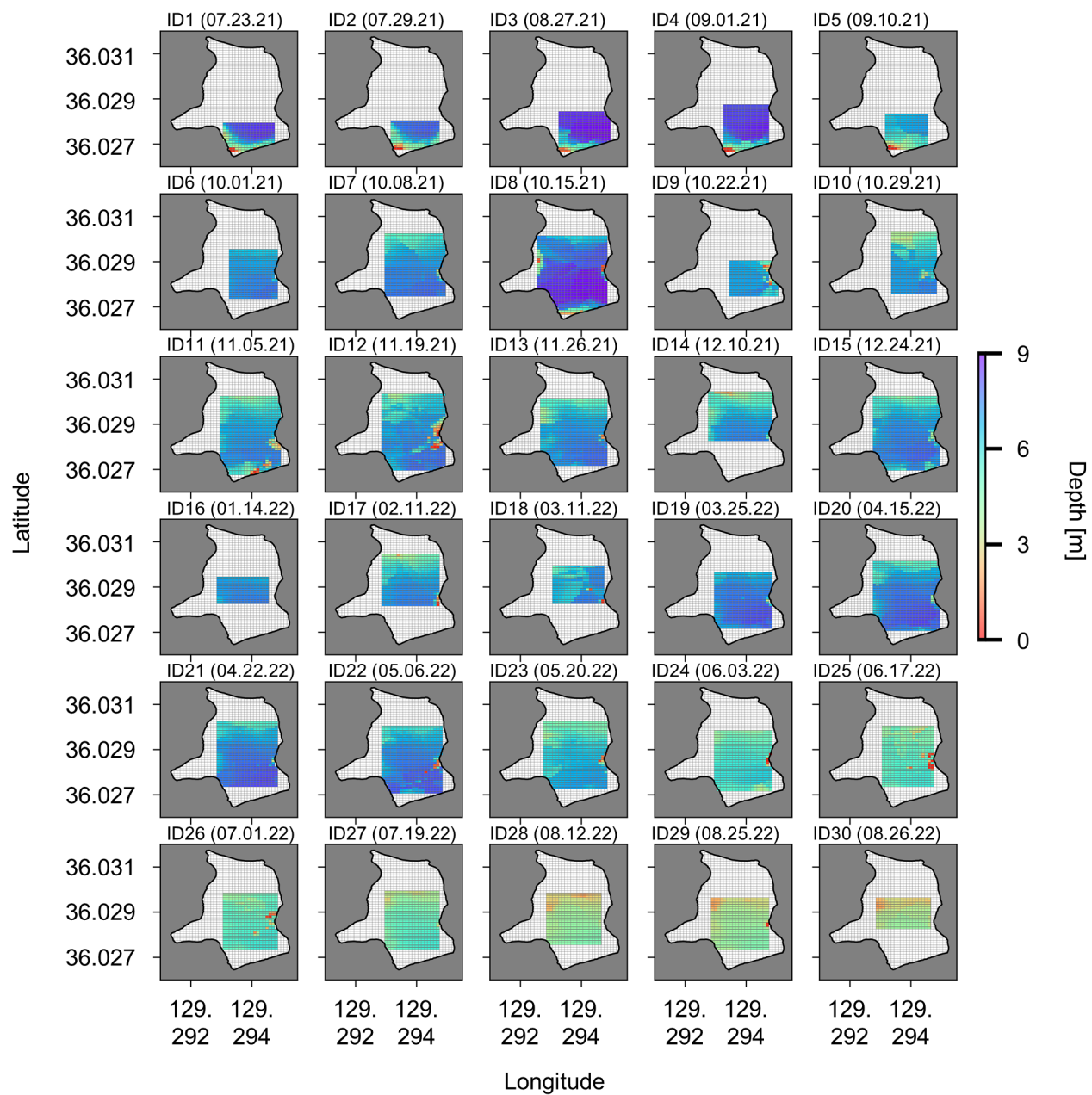


Figure 6.

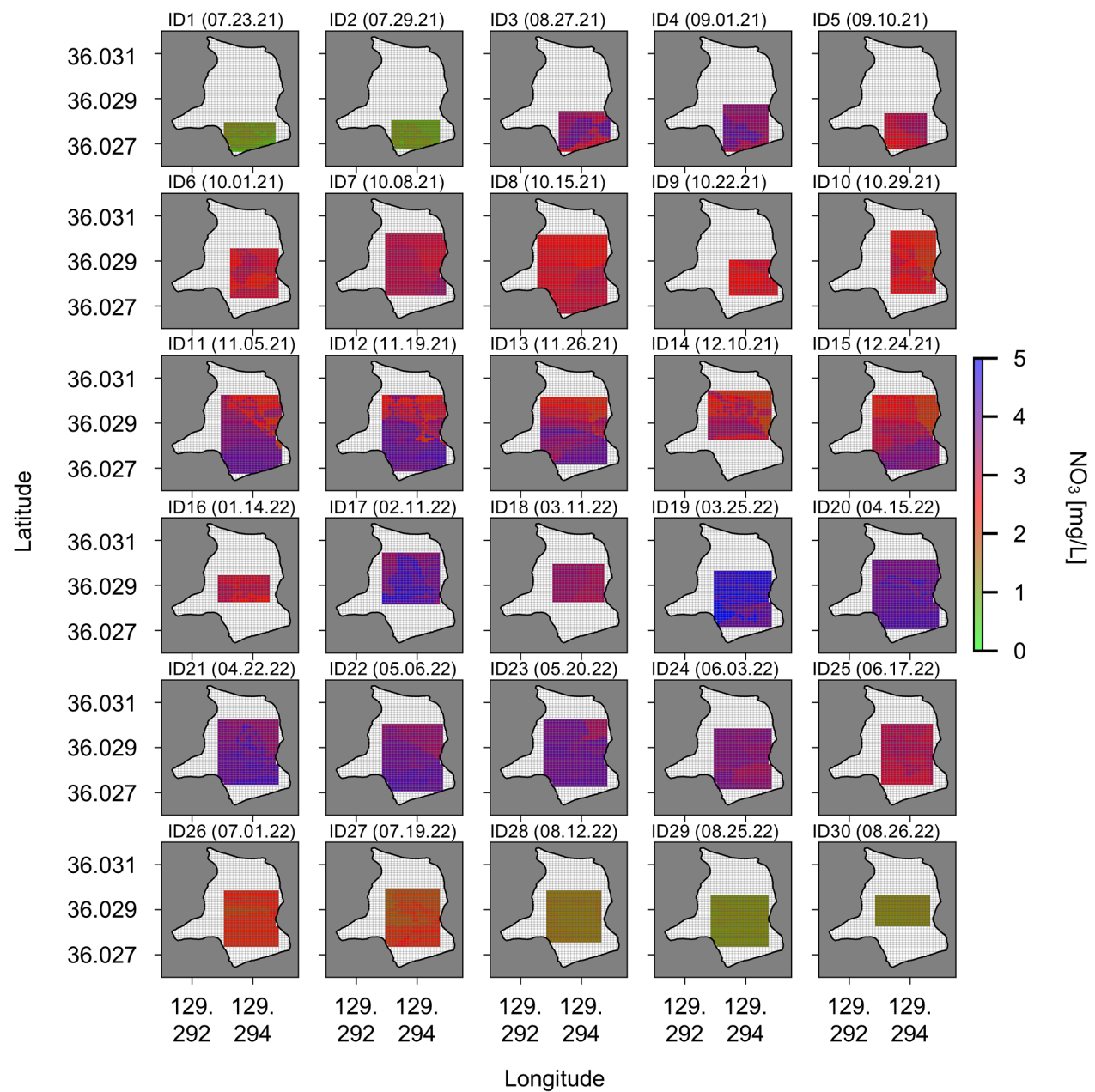


Figure 7.

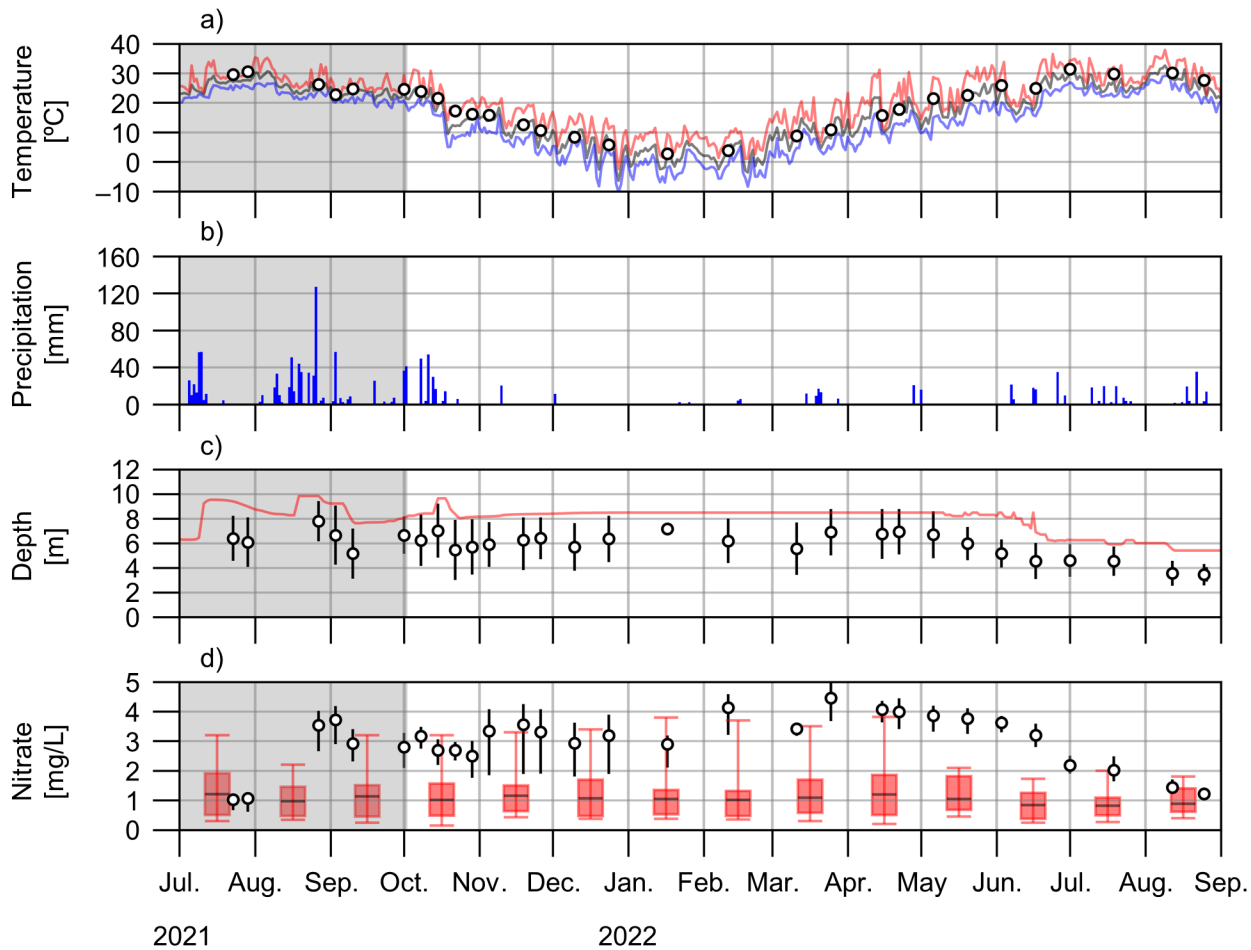


Figure 8.



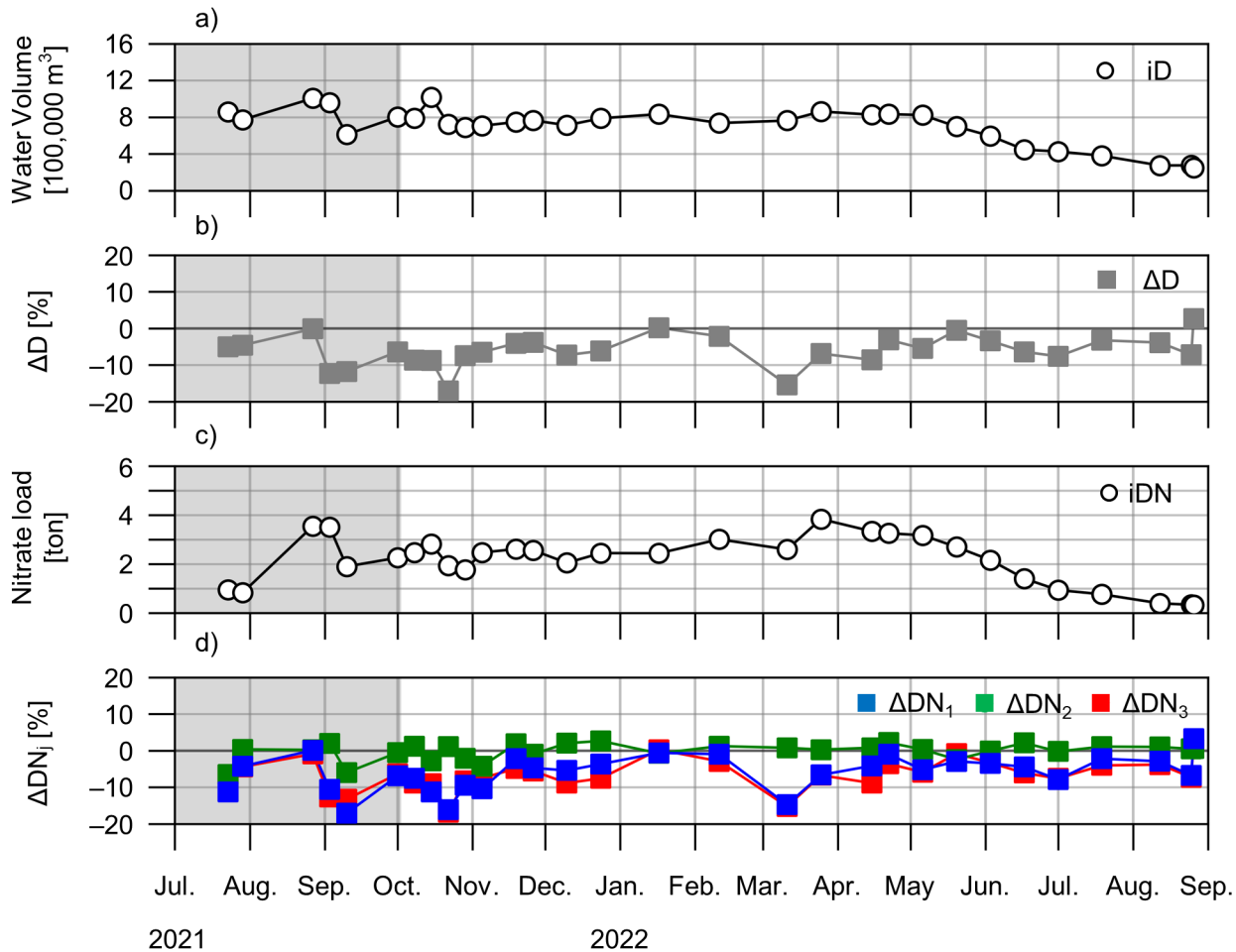


Figure 9.

